European Journal of Immunology Clinical·Basic·Translational

HIGHLIGHTS

Basic

FRONTLINE | Rapid Research Article

Single-cell fate mapping reveals widespread clonal ignorance of low-affinity T cells exposed to systemic infection

***Justin Leube*[#1], *Anton Mühlbauer*[#1], *Immanuel Andrä*[1], *Madleen Biggel*[1], *Dirk H. Busch*[1,2], *Lorenz Kretschmer*[##1] *and Veit R. Buchholz*[##1]**

[1] Institute for Medical Microbiology, Immunology and Hygiene, Technische Universität München (TUM), Munich, Germany
[2] German Center for Infection Research (DZIF), Munich, Germany

T cell ignorance is a specific form of immunological tolerance. It describes the maintenance of naivety in antigen-specific T cells in vivo despite the presence of their target antigen. It is thought to mainly play a role during the steady state, when self-antigens are presented in absence of costimulatory signals and at low density or to T cells of low affinity. In how far antigen-specific T cells can also remain clonally ignorant to foreign antigens, presented in the inflammatory context of systemic infection, remains unclear. Using single-cell in vivo fate mapping and high throughput flow cytometric enrichment, we find that high-affinity antigen-specific CD8$^+$ T cells are efficiently recruited upon systemic infection. In contrast, most low-affinity antigen-specific T cells ignore the priming antigen and persist in the naïve state while remaining fully responsive to subsequent immunization with a high-affinity ligand. These data establish the widespread clonal ignorance of low-affinity T cells as a major factor shaping the composition of antigen-specific CD8$^+$ T cell responses to systemic infection.

Keywords: single-cell fate mapping · T cell ignorance · T cell receptor affinity · T cell recruitment · T cell tolerance

Additional supporting information may be found online in the Supporting Information section at the end of the article.

Introduction

CD8 T cell responses are initiated by individual T cell clones, harboring unique T cell receptors (TCRs) that recognize their cognate antigen in the context of MHC-I [1]. Following TCR stimulation in concert with ligation of co-stimulatory and cytokine receptors, activated T cells vigorously proliferate and differentiate into short-lived terminal effectors (TEs) and long-lived memory precursors (MPs) [2–4]. CD62L$^-$CD27$^-$ TEs acquire potent antimicrobial functions, but succumb to apoptosis after pathogen clearance [3, 5], whereas CD62L$^+$CD27$^+$ Central memory precursors (CMPs) and CD62L$^-$CD27$^+$ Effector memory precursors (EMPs) persist long-term and develop into T central memory (T_{CM}) and T effector memory (T_{EM}) cells, respectively [6–8].

An important factor that influences CD8$^+$ T cell responses to infection or vaccination is the binding affinity of the TCR to its cognate peptide MHC-I ligand (p:MHC-I). TCR affinity for a given

Correspondence: Veit R. Buchholz and Lorenz Kretschmer
e-mail: veit.buchholz@tum.de; lorenz.kretschmer@tum.de

[#]These authors contributed equally
[##]Senior authors

© 2022 The Authors. *European Journal of Immunology* published by Wiley-VCH GmbH

This is an open access article under the terms of the Creative Commons Attribution-NonCommercial-NoDerivs License, which permits use and distribution in any medium, provided the original work is properly cited, the use is non-commercial and no modifications or adaptations are made.

p:MHC-I can vary considerably between the individual cells of an epitope-specific T cell population [1] and both high and low-affinity T cells can participate in primary and secondary $CD8^+$ T cell responses [9, 10]. However, it has long been noted that high-affinity T cells increasingly dominate the epitope-specific TCR repertoire throughout the course of primary and recall responses [11–15]. Both, the efficiency of T cell recruitment (i.e. the likelihood with which an antigen-specific T cell exits its naïve state) as well as the extent of T cell clonal expansion could contribute to regulating the magnitude of high- versus low-affinity T cell responses. Via single-cell fate mapping, it has been shown that systemic infection leads to near complete recruitment of high-affinity T cell clones [16]. Moreover, it has been found that during the course of infection even very low-affinity TCR p:MHC-I interactions result in some T cell expansion and the development of immunological memory [10]. The proliferation of low-affinity T cells stops earlier than that of high-affinity T cells and this differential expansion has been considered as the main factor regulating the progressive skewing of the TCR repertoire toward high-affinity clones [10]. However, the actual recruitment of single low-affinity T cells has not been investigated directly. Instead, the aforementioned study focused on immune responses derived from naïve T cell *populations*, making it impossible to answer, whether effective T cell expansion originated from many or only a few recruited clones.

Using single-cell *in vivo* fate mapping and high-throughput flow cytometric enrichment, we show here that, in accordance with previous findings [16], high-affinity TCR p:MHC-I interactions during systemic infection indeed recruit most epitope-specific T cells. However, low-affinity interactions leave the majority of epitope-specific T cells in an ignorant state, characterized by the maintenance of naivety and full responsiveness to subsequent high-affinity antigen challenge.

Generally, T cell ignorance is defined as the unresponsiveness of self-antigen specific T cells to their cognate ligand. Ignorance is maintained due to antigen sequestration behind a tissue barrier, antigen presentation at low density, or antigen recognition by T cells of low affinity [17]. T cells expressing high-affinity self-reactive TCRs rarely escape thymic deletion, and if so, remain ignorant only to very low antigen doses while otherwise TCR signaling in absence of co-stimulation drives them into anergy [18, 19]. Therefore, mainly low-affinity self-reactive T cells are maintained in an ignorant state, from which they are thought to be readily recruited in the costimulatory context of systemic infection [20, 21].

Our data now establish that while antigen exposure in the context of systemic infection indeed leads to expansion of low-affinity T cell populations, this expansion is based on the recruitment of only a minority of available epitope-specific T cells. The majority of these low-affinity T cells instead continues to ignore its cognate antigen and retain a naïve phenotype. These data translate the fundamental concept of T cell ignorance from a purely steady-state context to that of systemic infection and show that this tolerance mechanism is more stably maintained than previously assumed.

Results

Tracking $CD8^+$ T cell responses to high- or low-affinity antigen by *in vivo* single-cell fate mapping

To investigate the recruitment, expansion, and phenotypic diversification of $CD8^+$ T cells exposed to high-, medium-, or low-affinity TCR p:MHC-I interactions in the context of systemic infection, we made use of the bacterial pathogen *Listeria monocytogenes* expressing the SIINFEKL peptide of chicken Ovalbumin (Lm-N4) or an altered peptide ligand (APL) with medium (Lm-Y3) or low affinity (Lm-T4) to the OT-1 TCR [22]. We adoptively transferred either 100 OT-1 T cells or up to eight single OT-1 T cells each harboring a distinct congenic phenotype that allowed us to track multiple single-cell-derived immune responses in parallel within the same host (Fig. S1). After adoptive transfer, C57BL/6 recipients were infected with Lm-N4, Lm-Y3, or Lm-T4. Eight days after infection we measured the size and phenotypic composition of immune responses derived from 100 or single OT-1 T cells in spleens of recipient mice (Fig. 1A). As described previously [23, 24], stronger TCR stimulation led to an increase in T cell expansion and a relative decrease in CMP differentiation (Fig. 1B-C). However, expansion and phenotypic differentiation emerging from single T cells strongly varied and considerably overlapped between high, medium, and low-affinity TCR ligation, re-affirming the probabilistic nature of clonal T cell responses [25, 26] (Fig. 1B and C). Interestingly, when comparing APLs of distinct affinity, average response sizes of T cell populations differed substantially more than average expansion of T cell clones. In fact, average size of Lm-N4- versus Lm-T4-driven population-derived responses differed by 155-fold while average size of detectable T cell clones, expanded in response to Lm-N4 versus Lm-T4, differed by only 17-fold (Fig. 1B). This discrepancy was at least partially resolved by our finding that more than 60% of all transferred single T cells expanded into detectable clones upon Lm-N4 infection while only 20% of transferred single T cells did so upon Lm-T4 infection (Fig. 1D and E). This more than 3-fold lower recovery of expanded T cell clones in response to Lm-T4 vs. Lm-N4 did not result from differential competition with the endogenous T cell repertoire (Fig. S2A–C). In fact, absence of endogenous competition in T cell deficient $TCRalpha^{-/-}$ mice reduced the difference in clonal expansion (Fig. S2D–F) but left the fold-difference in clonal recovery between low- and high-affinity primed T cells virtually unchanged (Fig. S2G). Such clonal underrepresentation may be due to insufficient clonal expansion, and thus undetectability of activated T cells or due to the failure of naïve T cells to be activated at all. The latter process, termed clonal ignorance, is widely found for T cells recognizing self-antigens presented at low density and in absence of costimulation during the steady state [20, 21], however, it has not been described during infection.

© 2022 The Authors. *European Journal of Immunology* published by Wiley-VCH GmbH

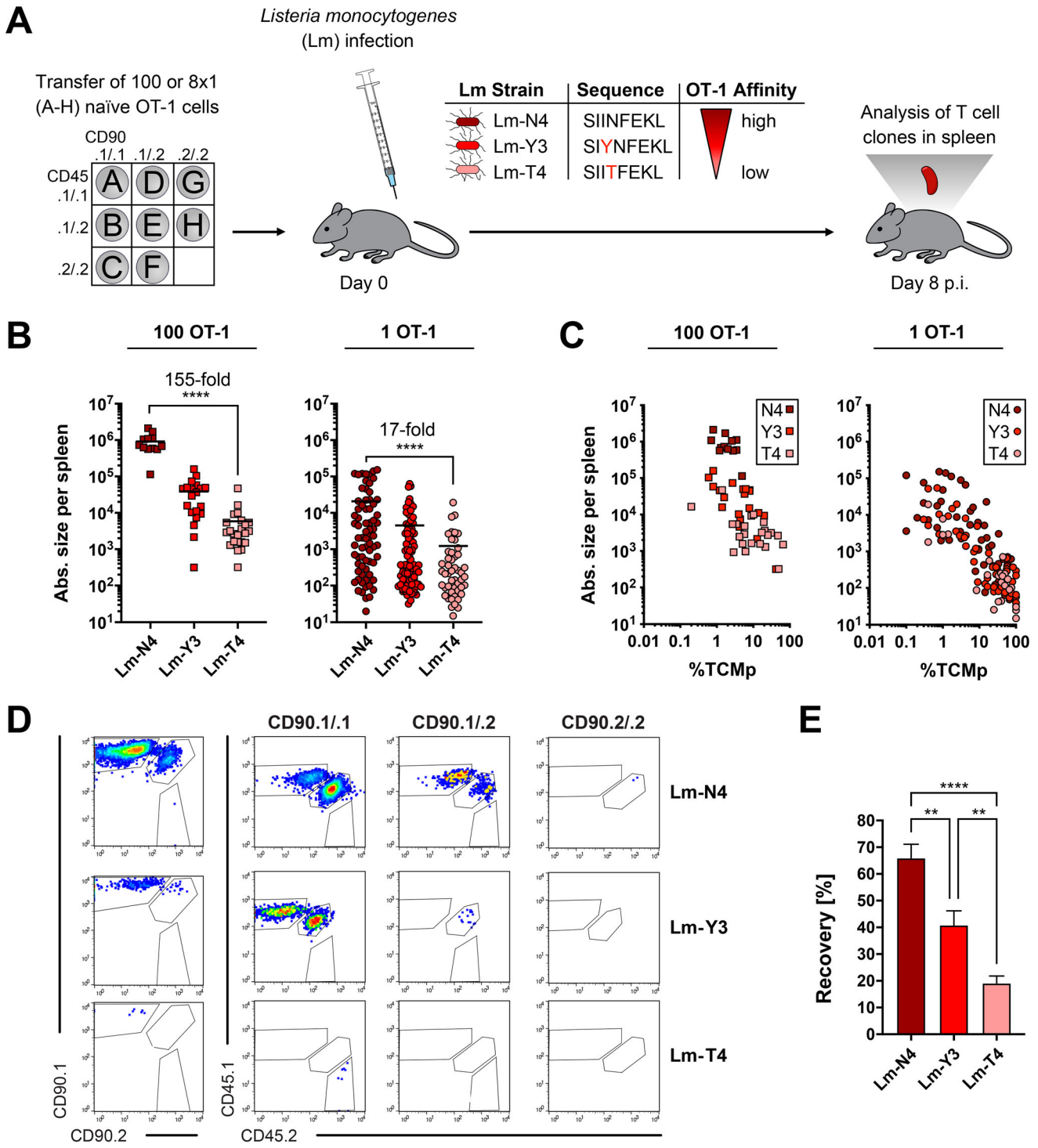

Figure 1. Recovery of single cell-derived CD8$^+$ T cell responses is reduced upon low-affinity T cell priming. (A) 100 or 8x1 naïve OT-1 T cells were transferred into C57BL/6 mice followed by infection with 5000 CFU Lm-N4, Lm-Y3 or Lm-T4. Analysis of expanded T cell populations was performed at day 8 post-infection. (B) Absolute cell numbers of 100 cell (left panel) and single-cell derived responses (right panel) in the spleen of recipient mice. (C) Correlation between absolute cell numbers and percentage of CMP cells for immune responses derived from 100 (left panel) or single naïve OT-1 T cells (right panel). (D) Representative pseudo-color plots showing the detection of single-cell-derived T cell responses after Lm-N4, Lm-Y3, and Lm-T4 infection. (E) Corresponding bar graph depicts the percentage of recovered single cell-derived T cell responses. One hundred cell-derived data are compiled from at least three experiments with at least $n = 4$ mice per group. Single-cell transfer data are compiled from four to five independent experiments with at least $n = 5$ mice per group. Lines indicate the mean, error bars the SEM. Significances are calculated using one-way ANOVA (Kruskal-Wallis) and Dunn's multiple comparison test. $^*P < 0.05$, $^{**}P < 0.01$, $^{***}P < 0.001$, $^{****}P < 0.0001$.

© 2022 The Authors. *European Journal of Immunology* published by Wiley-VCH GmbH

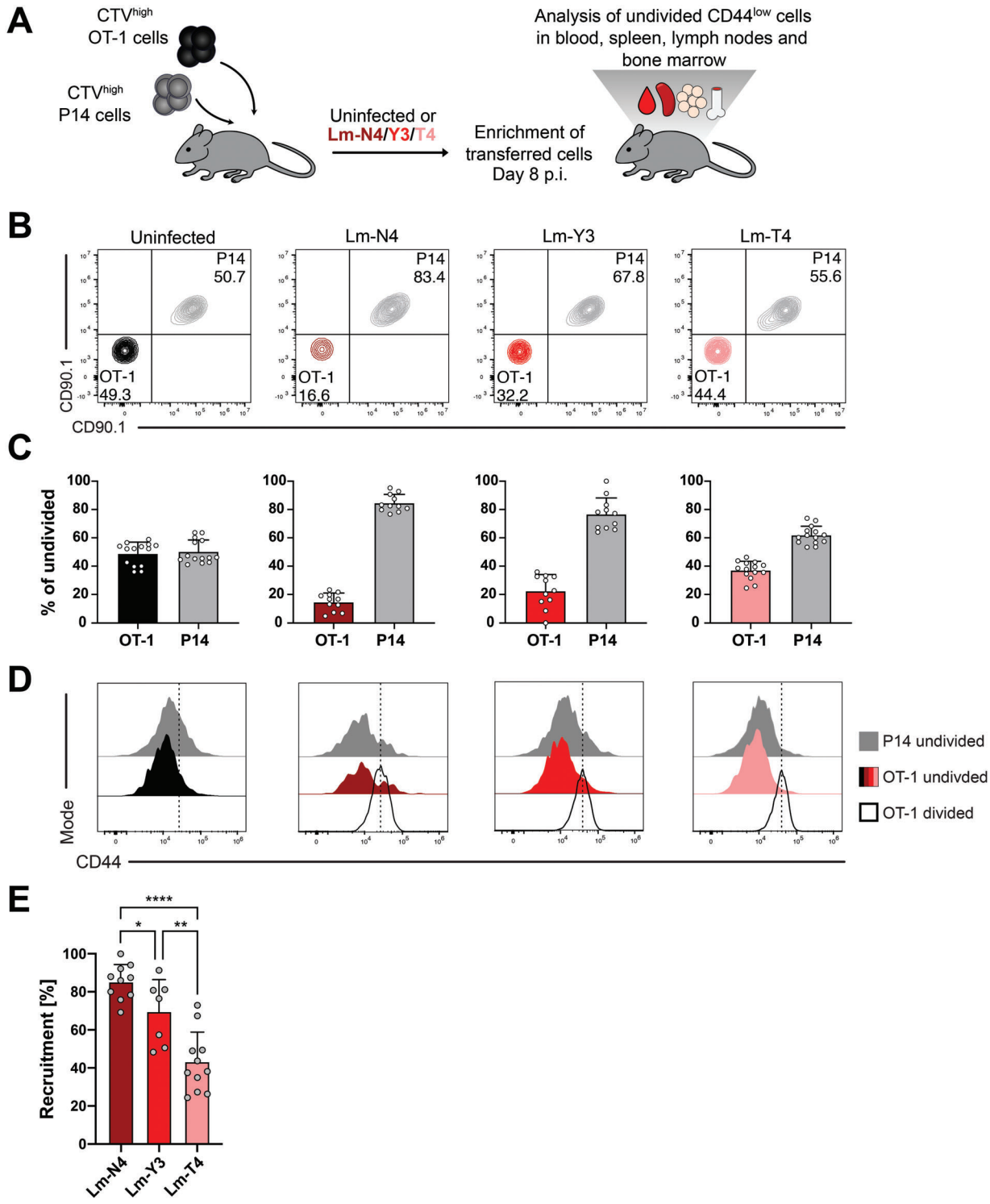

Figure 2. Low-affinity T cell priming leads to impaired recruitment of antigen-specific CD8$^+$T cells. (A) 2.5 × 10^4 CTV labeled naïve OT-1 (CD45.1$^+$ CD90.1$^-$) and P14 (CD45.1$^+$ CD90.1$^+$) cells were co-transferred into C57BL/6 mice followed by infection with 5000 CFU Lm-N4, Lm-Y3 or Lm-T4. On day 8 p.i. blood, spleen, lymph node, and bone marrow cells were enriched for CD45.1$^+$ cells and analyzed for the presence of unrecruited (undivided CD44^{low}) cells. (B) Representative contour plots showing the frequency of OT-1 and P14 cells among undivided CD45.1$^+$ CD44^{low} live CD8$^+$ T cells. (C) Bar graphs show the percentage of OT-1 and P14 cells among undivided CD44^{low} live CD8$^+$ T cells. (D) Histograms depict CD44 expression among undivided P14, undivided OT-1, and divided OT-1 T cells. The dotted line indicates the CD44 geo-MFI of the OT-1 divided population. For the uninfected setting, the CD44 geo-MFI values of the N4 setting were used. (E) Bar graphs depict the efficiency of T cell recruitment, calculated from the measured OT-1 to P14 ratios from infected and uninfected mice shown in (B) and (C). Data are compiled from four independent experiments with n = 3 mice per group. Lines indicate the mean, error bars the SD (C) or SEM (E). Significances in are calculated using one-way ANOVA (Kruskal-Wallis) and Dunn's multiple comparison test. *$P < 0.05$, **$P < 0.01$, ***$P < 0.001$, ****$P < 0.0001$.

© 2022 The Authors. *European Journal of Immunology* published by Wiley-VCH GmbH

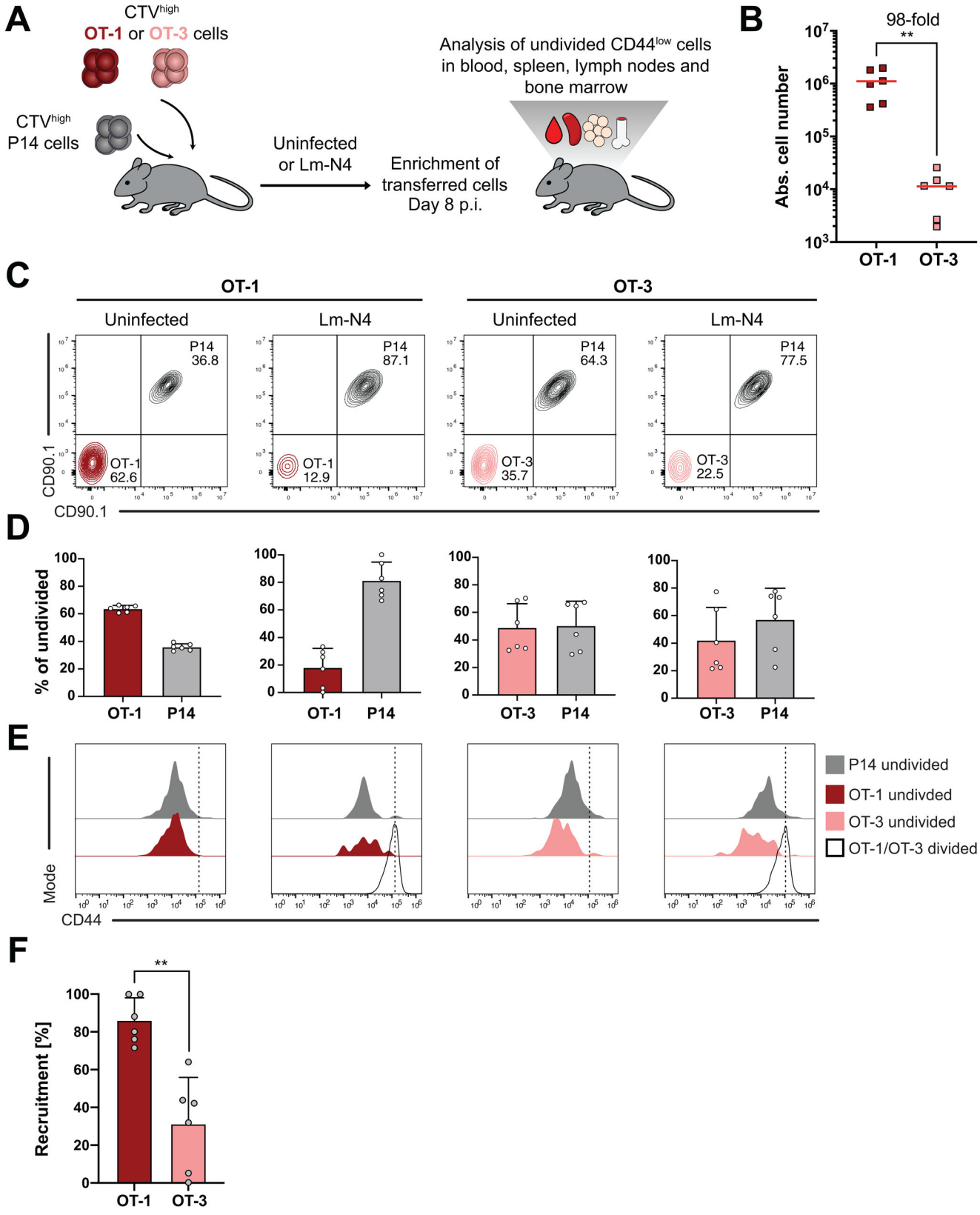

Figure 3. T cells harboring TCRs of low affinity are incompletely recruited during primary immune responses. (A) 2.5 × 10^4 CTV labeled naïve OT-1 or OT-3 (CD45.1$^+$ CD90.1$^-$) were co-transferred with 2.5 × 10^4 CTV labeled naïve P14 (CD45.1$^+$ CD90.1$^+$) cells into C57BL/6 mice followed by infection of recipients with 5000 CFU Lm-N4. On day 8 p.i. blood, spleen, lymph nodes, and bone marrow cells were enriched for CD45.1$^+$ cells and

© 2022 The Authors. *European Journal of Immunology* published by Wiley-VCH GmbH

Recruitment of antigen-specific CD8$^+$ T cells is impaired upon low-affinity T cell priming

Thus, to follow up on our initial finding, we more directly investigated the maintenance of T cell ignorance—not by measuring the number of recruited and expanded clones but by measuring the number of individual cells left unrecruited upon infection. To achieve this, we labeled OT-1 and P14 T cells (the latter being specific to the glycoprotein antigen of Lymphocytic choriomeningitis virus) [27], with a division tracking dye and adoptively transferred these to hosts exposed to Lm-N4, Lm-Y3 or Lm-T4 infection. We then harvested lymphoid organs on day 8 after infection and utilized a high throughput flow cytometry-based approach for speed-enrichment of congenic marker-expressing cells (see Materials and Methods for details). Among these we then measured the number of T cells that remained undivided at day eight post-infection in both the antigen-specific and antigen-unspecific T cell population (Fig. 2A). Using this approach, we found that the percentage of OT-1 vs. P14 T cells among undivided cells at day 8 post-infection increased from Lm-N4 to Lm-Y3 to Lm-T4 (Fig. 2B–C and Fig. S3A–B). Importantly, these undivided T cells all remained CD44^{low} and, thereby, phenotypically naïve (Fig. 2D). To test the developmental potential of these unrecruited T cells, we transferred them together with bona fide naïve T cells into uninfected secondary hosts, which we infected 28 days later with modified vaccinia Ankara encoding for the target antigen Ovalbumin (MVA- OVA) (Fig. S4A–B). Importantly, after immunization with this viral vaccine vector, we found no differences between immune responses generated by unrecruited or naïve T cells, arguing that both populations share a similar developmental potential (Fig. S4C–E). Taken together, these observations indicate that recruitment was significantly decreased in T cells exposed to Lm-T4 versus Lm-Y3 versus Lm-N4 infection (Fig. 2E). To further corroborate this finding without relying on APLs, we made use of OT-3 T cells which express a transgenic TCR that binds the N4 peptide in the context of H-2K^b with similar affinity as the OT-1 TCR binds to the T4 APL [28]. By adoptively transferring either OT-1 or OT-3 T cells together with P14 T cells, which served as internal control, and harvesting spleen, lymph nodes, blood, and bone marrow at day 8 p.i. (Fig. 3A), we recapitulated our findings made with OT-1 T cells stimulated either with N4 peptide or APLs (Fig. 3B). Comparing uninfected with Lm-N4 infected mice, we found that the percentage of undivided, CD44^{low} T cells in antigen-specific versus antigen-unspecific T cells was strongly decreased for OT-1 versus P14 T cells while it remained almost unchanged for OT-3 versus P14 T cells (Fig. 3C–E). Accordingly, recruitment was significantly lower for OT-3 compared to OT-1 T cells (Fig. 3F). This indicated that even during systemic infection most low-affinity T cells ignored the priming antigen and only a minor fraction was activated and induced to proliferate.

Tracking the fate of unrecruited T cell clones upon secondary challenge

While lack of proliferation and absence of CD44 expression in these population-based experiments pointed towards clonal ignorance, we wanted to further investigate, whether individual T cells that remained un-recruited during primary infection indeed retained their full activation potential during a secondary challenge, thereby, further corroborating the operational definition of clonal ignorance. To achieve this, we analyzed immune responses derived from single OT-1 T cells longitudinally—first, after an initial infection with Lm-N4 or Lm-T4 and then again after a second infection with MVA-OVA. To make this analysis more efficient, we combined our congenic approach [25] and our recently developed retroviral color- approach [29, 30], thereby, enabling highly multiplexed single-cell transfer and response tracking. In brief, we utilized five OT-1 strains, expressing distinct congenic marker combinations, and introduced a diverse retroviral color-barcode into Sca-1$^+$ hematopoietic stem cells (HSCs) harvested from each of these strains. After combinatorial transduction with multiple fluorophore constructs, HSCs were transplanted into irradiated recipients, and approximately six weeks later yielded 10–20 discernable color-barcodes present in the hematopoietic compartment of each of the five congenically distinct chimeras. This then allowed us to adoptively transfer up to 85 color-congenic single OT-1 T cells into the same C57BL/6 recipient and track the presence of expanded clones upon subsequent infection (Fig. 4A). From our previous studies, we knew that while blood sampling is not sensitive enough to detect all recruited clones, even at the height of the primary immune response, clone detection via operative hemi-splenectomy is highly efficient [6]. We first confirmed that nearly all expanded T cell clones during Lm-N4 or Lm-T4 infection could indeed be recovered when sampling less than half of all splenocytes (4×10^7 cells) (Fig. S5A). Importantly, while detection rates slightly decreased upon sampling of fewer splenocyte numbers, these technical detection rates were very similar upon priming with Lm-N4 (82% detected) and Lm-T4 (84% detected) (Fig. S5B-C). On this basis, we then performed hemi-splenectomies eight days after the first infection with Lm-N4 or Lm-T4 and measured the size of expanded T cell clones. We

analyzed for the presence of unrecruited (undivided CD44^{low}) cells. (B) Absolute cell numbers of recovered OT-1 and OT-3 cells after enrichment. (C) Representative contour plots showing the frequency of OT-1, OT-3, and P14 cells among undivided CD45.1$^+$ CD44^{low} live CD8$^+$ T cells. (D) Bar graphs show the percentage of OT-1, OT-3, and P14 cells among undivided CD45.1$^+$ CD44^{low} live CD8$^+$ T cells. (E) Histograms depict CD44 expression among undivided P14, undivided OT-1 or OT-3, and divided OT-1 or OT-3 T cells. The dotted line indicates the CD44 geo-MFI of the OT-1 or OT-3 divided population. For the uninfected setting, the CD44 geo-MFI values of the corresponding OT-1 or OT-3 divided setting were used. (F) Bar graphs depict the efficiency of T cell recruitment, calculated from the measured OT-1 or OT-3 to P14 ratios from infected and uninfected mice shown in (C) and (D). Data are compiled from two independent experiments with $n = 3$ mice per group. Lines indicate the mean, error bars the SD (D) or SEM (F). Significances in (F) are calculated using t-test (Mann–Whitney). $^*P < 0.05$, $^{**}P < 0.01$, $^{***}P < 0.001$, $^{****}P < 0.0001$.

© 2022 The Authors. European Journal of Immunology published by Wiley-VCH GmbH

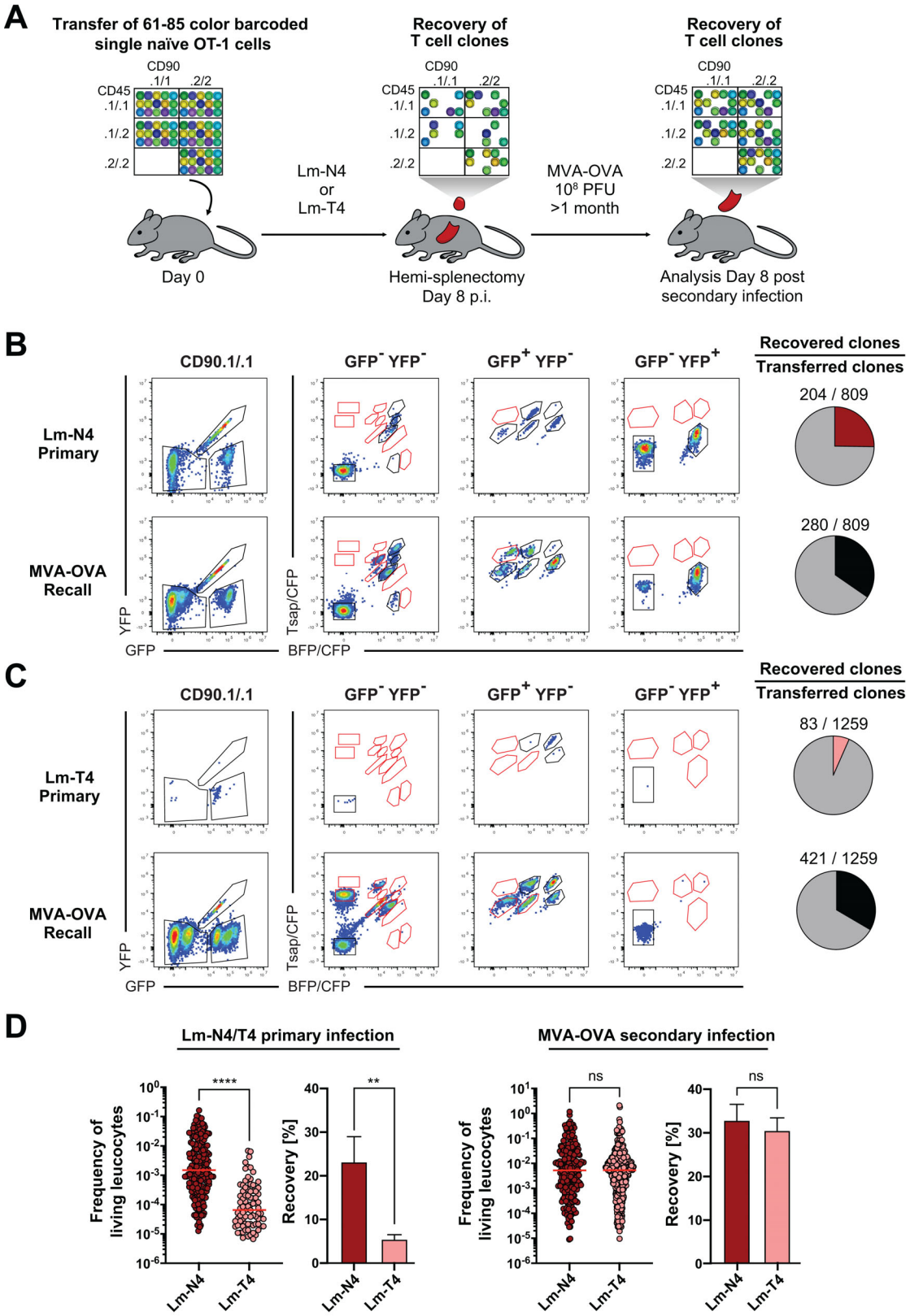

Figure 4. T cell clones that are left unrecruited during a primary infection can enter immune responses to a secondary high-affinity challenge. (A) 61–85 uniquely barcoded single naïve OT-1 T cells were transferred into CD11c-DTR-GFP recipients followed by infection with 5000 CFU Lm-N4 or Lm-T4. Recovery and size of individual T cell clones were initially assessed by hemi-splenectomy on day 8 p.i. Secondary responses within the same recipients were then assessed on day 8 after a heterologous challenge with 10^8 PFU MVA-OVA. (B) Quantification and representative pseudo color

© 2022 The Authors. *European Journal of Immunology* published by Wiley-VCH GmbH

then waited at least one month, then performed a second infection with MVA-OVA and measured the size and number of previously recovered vs. newly detected T cell clones (Fig. 4A). Of the 809 single OT-1 T cells transferred in total and exposed to initial high-affinity priming, we recovered 204 expanded clones at day 8 after Lm-N4 infection and 280 after subsequent MVA- OVA infection (Fig. 4B and Fig. S6A). Of the 1259 single OT-1 T cells transferred in total and exposed to initial low-affinity priming, we recovered 83 at day 8 after Lm-T4 infection and 421 after subsequent MVA-OVA infection (Fig. 4C and Fig. S6B). Importantly, the percentage of detected T cell clones that had been significantly lower after Lm-T4 vs. Lm-N4 infection, increased to the same maximum level in both groups in response to the second MVA-OVA infection (Fig. 4D). This argued that those single T cells that had remained un-recruited during the first infection were readily able to enter the immune response against a second high-affinity challenge. As shown previously for population-derived immune responses [10], we found that clonal response sizes to Lm-N4 vs. Lm-T4 infection were highly distinct while average expansion of T cell clones in response to a second infection with a heterologous vector expressing the high-affinity antigen (i.e. MVA-OVA) was virtually identical (Fig. 4D). However, response composition was clearly distinct, with 36% vs. 82% of T cell clones being newly detected in response to the second infection with MVA-OVA in the groups that had been exposed to initial infection with Lm-N4 vs. Lm-T4, respectively (Fig. 5A). As expected, these newly detected clones showed significantly smaller median expansion compared to initially recruited and then recalled clones. More importantly, the expansion size of newly detected clones at day 8 after the second MVA-OVA infection was indistinguishable from that of single naïve T cells responding to primary MVA-OVA challenge (Fig. 5B), thus, further supporting the hypothesis that clones, newly detected upon MVA-OVA infection, indeed originated from T cells that had remained ignorant to initial priming. Interestingly, we found that a minor fraction of T cells exposed to high-affinity priming also remained ignorant and entered the response only upon renewed infection. The contribution of these initially ignorant high-affinity primed T cells to the clonal composition and overall magnitude of secondary immune responses was, however, substantially smaller than that of T cells exposed to low-affinity priming (Fig. 5C). Taken together, our data indicate that T cell responses to renewed antigen challenge are composed of bona fide recalled clones and newly recruited naïve T cells that had remained ignorant to initial priming. Importantly, this ignorance is particularly widespread if initial TCR p:MHC-I interactions are of low-affinity.

Discussion

It has been previously suggested that the recruitment of single antigen-specific $CD8^+$ T cells upon systemic pathogen challenge is virtually complete [16]. This prior study, however, focused on primary clonal expansion of single T cells in response to high-affinity TCR p:MHC-I interactions. Here, we instead analyzed the clonal expansion of single antigen-specific T cells in response to both high- and low-affinity priming and further assessed completeness of initial T cell recruitment by performing a secondary challenge with a heterologous vaccine vector encoding the high-affinity antigen. This two-pronged approach revealed that the majority of T cell clones that participated in the response to secondary infection had remained ignorant to initial low-affinity priming. Moreover, a small fraction of T cell clones also ignored initial high-affinity priming and entered the response only upon secondary infection. These findings reveal that the increasing dominance of high- vs. low-affinity T cell clones during infection or vaccination is not only governed by their differential expansion [10, 11, 14] and contraction [31] but also by their affinity-dependent recruitment. While indeed very low-affinity TCR p:MHC-I interactions can lead to expansion and memory differentiation of $CD8^+$ T cells [10], they do so in only a minor fraction of naïve T cells exposed to low-affinity priming. T cell clones that successfully expand under these conditions are then fully equivalent in their recall capacity to T cell clones that were initially expanded in response to high-affinity priming. However, the likelihood of such effective recruitment is strongly reduced upon low-affinity engagement. Such all-or-non response patterns have recently also been reported upon *in vitro* activation of $CD8^+$ T cells. In the respective study high- vs. low-affinity TCR p:MHC-I interactions lead to more efficient and uniform T cell activation. However, once activated, high- and low-affinity-primed T cells both acquired full cytolytic capacity [32].

Further on, our work shows that clonal ignorance, i.e., the preservation of a naïve T cell phenotype despite the presence of the target antigen, is not reserved to self-antigens presented at low density and in the absence of inflammatory stimuli during the steady state but also occurs in the majority of low-affinity T cells exposed to their foreign antigen in the costimulatory context of systemic infection. Importantly, the OT-1 TCR interaction with the T4 ligand, that we have investigated here, has been previously shown to lie at the threshold beyond which thymic deletion is initiated – given that the T4 ligand is expressed as a quasi-self-antigen in the thymi of OT-1 TCR transgenic mice [33]. This threshold affinity of a TCR to self-antigen is considered particularly dangerous for induction of autoimmunity, since it induces

plots showing detection of T cell clones on day 8 after primary infection with Lm-N4 (upper row) and post MVA-OVA challenge (lower row). (C) Same as is (B), but for primary infection with Lm- T4. (B and C) T cell clones were distinguished by their combinatorial color-congenic barcode: first by gating on their congenic marker combination and then and then their unique color-barcode (GFP and YFP (left) followed by BFP/CFP and T-Sap/CFP (right)). Note: the 90.1/.1 population displayed in this figure contained only unique color-barcodes and was therefore not further segregated into CD45.1/.1 and CD45.1/.2 subpopulations (a gating strategy containing all congenic-color combinations is included in Fig. S4). Red gates represent barcodes of transferred single cells, where no progeny was recovered in the shown recipient on day 8 p.i. Pie charts show the ratio of recovered to transferred single T cells. (D) Scatter plots depicting the response size and bar graphs depicting the percentage of recovered single T cell clones after primary infection (left panel) and after secondary infection (right panel). Data are compiled from five independent experiments with $n = 3$ mice in the Lm-N4 and $n = 4$ mice in the Lm-T4 group. Lines in the scatter plot indicate the median, bar graphs indicate the mean and SEM. Significances in (C) are calculated using *t*-test (Mann–Whitney). $^*P < 0.05$, $^{**}P < 0.01$, $^{***}P < 0.001$, $^{****}P < 0.0001$.

© 2022 The Authors. *European Journal of Immunology* published by Wiley-VCH GmbH

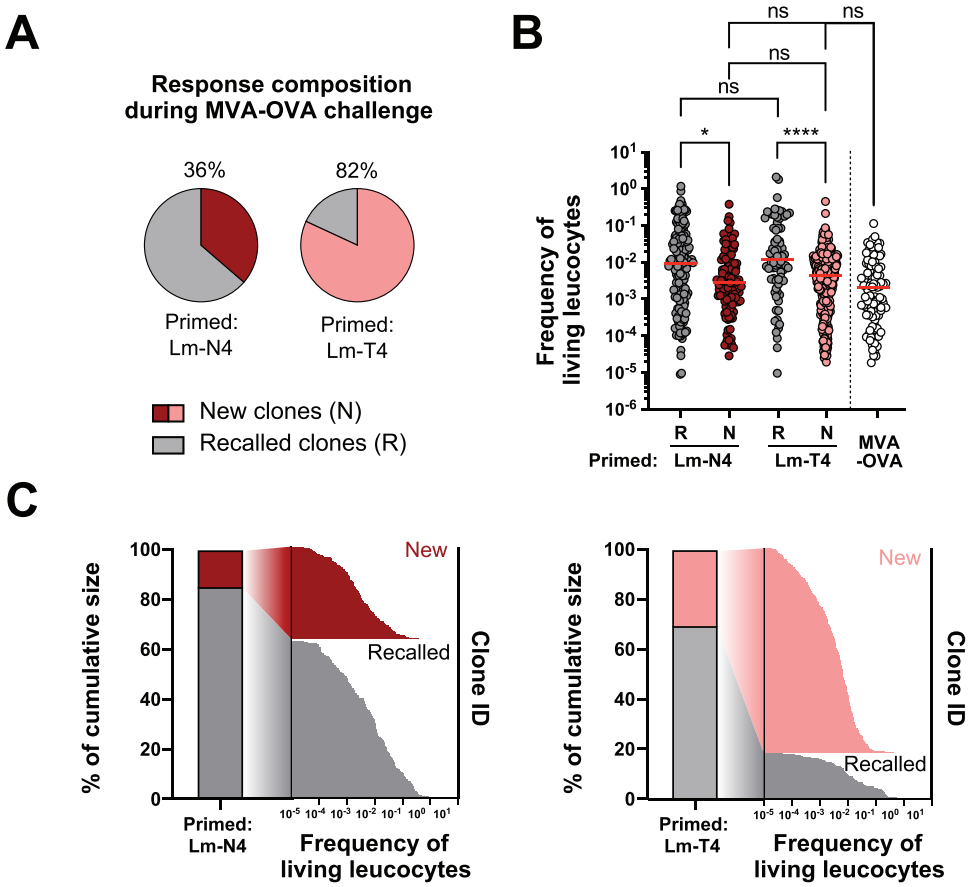

Figure 5. Secondary responses after low-affinity T cell priming are mainly composed of newly recruited T cell clones. The data shown in this figure corresponds to the experiments described in Fig. 4. (A) Pie charts show the percentage of recalled (R) and newly recruited (N) clones after secondary MVA-OVA infection. (B) Response size of recalled and newly recruited T cell clones in comparison to single cell-derived primary responses to MVA-OVA infection. (C) Contribution of newly recruited and recalled clones to cumulative response size and clonal composition after Lm-N4 (left) or Lm-T4 priming (right). The bar graphs show the contribution of recalled and newly recruited clones to the cumulative response size of all recovered T cell clones (left y-axis). The line graphs show the response size of each detected clonal response (x-axis), as well as the number of detected responses (right y-axis). Clones are colored according to their status as new clones or recalled clones. Data are compiled from five independent experiments with $n = 3$ mice in the Lm-N4 and n = 4 mice in the Lm-T4 group and two independent experiments with $n = 8$ mice (MVA-OVA primary). Lines indicate the median. Significances in (B) are calculated using one-way ANOVA (Kruskal–Wallis) and Dunn's multiple comparison test. $^{*}P < 0.05$, $^{**}P < 0.01$, $^{***}P < 0.001$, $^{****}P < 0.0001$.

little thymic deletion or peripheral tolerance via induction of T cell anergy [34]. Instead, it allows for the thymic exit of low-affinity self-reactive naïve T cells that remain ignorant to self-antigen during the steady state but are considered to be fully responsive to it when it is presented in the context of infection. However, data showing efficient expansion of low-affinity T cells during infection have until now only relied on population-based experiments [10]. By mapping the fate of *single* antigen-specific T cells *in vivo*, we show here that the recruitment of low-affinity $CD8^+$ T cells into an adaptive immune response to infection is in fact a rare event.

It has been shown that breaching tolerance in mice expressing OVA in the thymus and the pancreas via infection with OVA-expressing pathogens, will lead to the expansion of OVA-specific $CD8^+$ T cells harboring TCRs at the threshold of thymic deletion. This expansion of autoreactive T cells, however, does not occur readily upon primary infection and instead, even repetitive immunization leads to type 1 diabetes development in only a sub-fraction of exposed mice [28]. Our findings suggest that this breach of tolerance may be so rare due to ignorance being more stably maintained in low-affinity T cells than previously expected.

Taken together, our work identifies widespread clonal ignorance of low-affinity $CD8^+$ T cells in the context of systemic infection. This finding may provide a better understanding of the equilibrium between thymic deletion and the maintenance of immune tolerance. In fact, it is tempting to speculate that the threshold of thymic deletion may be evolutionarily tailored so that most $CD8^+$ T cells with a TCR affinity to self-antigen just low enough to escape thymic deletion, will maintain their ignorance to self-antigen not only during the steady-state but also in the context of systemic infection—making the breach of clonal ignorance a dangerous but rare event.

© 2022 The Authors. *European Journal of Immunology* published by Wiley-VCH GmbH

Materials and methods

Mice

C57BL/6JOlaHsd mice were purchased from Envigo. SIINFEKL peptide-specific TCR transgenic OT-1 (C57BL/6-Tg(TcraTcrb)1100Mjb/J, CD45.1 (B6.SJL-Ptprca Pepcb/BoyJ), CD90.1 (B6.PL-Thy1^{a}/CyJ), TCRalpha$^{-/-}$ (B6.129S2Tcra< tm1Mom>/J) and CD11c-DTR (B6.FVB-Tg(Itgax-DTR/EGFP)57Lan/J) mice were originally obtained from The Jackson Laboratory and bred under specific pathogen-free conditions at the mouse facility of the Technical University of Munich. OT-1 mice were crossed to a Rag1$^{-/-}$ and diverse congenic background as previously described (OT-1 Rag-1 $^{-/-}$ Matrix mice) [25]. OT-3 TCR GFP mice were kindly provided by Dietmar Zehn (Technical University of Munich, Germany). Age- and sex-matched recipient mice were used at an age of 6–12 weeks for transfer and infection experiments. Donor mice were used at an age from 6 to 24 weeks.

Infections

Mice were infected intravenously with 5000 CFU recombinant *Listeria monocytogenes* expressing SIINFEKL (N4), SIYNFEKL (Y3) or SIITFEKL (T4). Heterologous recall was performed by intraperitoneal infection with 10^{8} PFU recombinant Modified Vaccinia Ankara (MVA) Virus expressing Ovalbumin (OVA).

Tissue culture

The Platinum-E packaging cell line was cultured in DMEM (Life Technologies), supplemented with 10% FCS, 0.025% L-glutamine, 0.1% HEPES, 0.001% gentamycin, and 0.002% streptomycin (cDMEM).

Generation of retrovirus for color barcoding

Retrovirus was produced as described by [29, 30]. In brief, Platinum-E packaging cells were transfected via calcium phosphate precipitation with retroviral vectors (MP71, a kind gift from Prof. W. Uckert, Berlin, Germany) encoding for five fluorescent proteins (GFP, YFP, CFP, BFP, and Ametrine). 48 and 72 hours after transfection the supernatant of the Platinum-E cells was collected and purified from the remaining cells by centrifugation at 800 xg at 4°C for 7 min. The supernatant was stored at 4°C and used within 4 weeks of collection.

Retrogenic mice

Retrogenic mice were generated as described by [29, 30]. In brief, bone marrow was collected from the tibia and femur of 10–16 week-old OT-1 Rag-1 $^{-/-}$ Matrix mice. The cells were brought into single-cell suspension and red blood cells were lysed. Subsequently, staining was performed with anti-mouse Ly6A/E (Sca-1) and anti-mouse CD19 antibodies. Propidium iodide was used for live/dead discrimination. Sorted Sca-1-positive 19-negative cells were incubated at 37°C in stimulation medium (cDMEM, supplemented with 20 ng/ml murine IL-3 (Preprotech), 50 ng/ml murine IL-6 (Preprotech) and 50 ng/ml murine SCF (Preprotech)), for 4 days in a tissue culture-treated 48-well plate (250,000–350,000 cells per 400 ml). Retroviral transduction with a fluorescent barcode was achieved by spinoculation. In brief, 400 μl of the combined Platinum-E supernatants were centrifuged at 3,000*g* and 32°C for 2 h in a tissue culture-untreated 48-well plate coated with RetroNectin (Takara, Japan) according to the manufacturer's instructions. Afterward, the supernatant was discarded, and the stem cells were added in stimulation medium at a concentration of 300,000 cells per 400 ml per well. Cells were then spinoculated at 800*g* at 32°C for 1.5 h. After 2 days in culture, the transduced stem cells were washed with cDMEM and injected i.v. into irradiated C57BL/6 recipient mice (4.5 Gy, twice with a resting period of 4 hours) at a dose of 500,000–1,000,000 cells in 100 μl FCS.

Flow cytometry

Single-cell suspensions were obtained by mashing collected tissues (spleen/lymph nodes/bone marrow) through a 70 μm cell strainer. Erythrocytes were lysed with ACT Buffer from spleen and blood samples. Cells were incubated with anti-CD16/CD32 for 30 min at 4°C and then washed with FACS buffer (PBS with 0.5% BSA and 2 mM EDTA). Afterward, cells were stained with respective antibodies from the following list for 30 minutes at 4°C: anti- CD8alpha (53-6.7, 5H10), anti-CD44 (IM7), anti-CD45.1 (A20), anti-CD90.1 (OX7, HIS51), anti-CD90.2 (53-2.1), anti-CD27 (LG7.F9), anti-CD19 (ID3), anti-CD62L (MEL-14), anti-CD45.2 (104), anti-Ly6A/E (D7). Live/Dead discrimination was performed by staining with Propidium iodide (Thermo Fischer) or Fixable Viability Dye eFluor™ 780 (Invitrogen). After washing with FACS buffer, the cells were analyzed using a Cytoflex S (Beckman Coulter), Cytoflex LX (Beckman Coulter) or CyAn ADP 9 color (Beckman Coulter) flow cytometer. Summit (v.4.3; Beckman Coulter) and FlowJo (v.9.6 and v.10.4; Becton Dickinson) were used for data acquisition and analysis, respectively.

Adoptive T cell transfer and tracking of single-cell-derived T cell responses

For adoptive transfer of single Rag-1$^{-/-}$ OT-1 T cells, peripheral blood mononuclear cells from retrogenic or congenic donor mice were stained following red blood cell lysis with antibodies directed against CD8 and CD44 (and CD45.1/CD90.1 when sorting from retrogenic mice). Propidium iodide was added dur-

© 2022 The Authors. *European Journal of Immunology* published by Wiley-VCH GmbH

ing sort for live/dead discrimination. Multiple single naïve T cells of distinct congenic phenotype or distinct color barcode (Living $CD8^+$ $CD44^{low}$) were sorted into a 96-well V-bottom plate containing a cell pellet of 4×10^5 C57BL/6 splenocytes in FCS. Cells were injected i.p. into C57BL/6 or C57BL/6-CD11c-DTR-GFP mice. As described previously [6], C57BL/6-CD11c-DTR-GFP mice were used for tracking fluorescently color- barcoded T cells, since this mouse strain is tolerant to transferred cells expressing members of the GFP-family proteins. Adoptive transfers for single T cell fate mapping were performed in a multiplexed fashion. This means that up to 8×1 T cells harboring distinct congenic marker profiles or up to 85×1 distinctively color-barcoded T cells were sorted into the same well and transferred in parallel into the same recipients. For population experiments 100 naïve OT-1 cells were transferred. Cell sorting was performed on a BD FACSAria III (Becton Dickinson), MoFlo XDP or MoFlo Astrios cell sorter (Beckman Coulter). Upon sample processing as described under "flow cytometry", single-cell-derived T cell responses were discriminated by congenic markers and/or retrogenic color barcodes.

Measurement of T cell recruitment

Splenocytes of OT-1, OT-3 (both $CD45.1^+$ $CD90.1^-$) and P14 ($CD45.1^+$ $CD90.1^+$) mice were stained with CellTrace violet (CTV, Invitrogen) according to manufacturer instructions and stained with monoclonal antibodies as described above. Respectively, 2.5×10^4 $CD8^+$ $CD44^{low}$ CTV^{high} OT-1 or OT-3 cells were cotransferred with P14 cells into C57BL/5 ($CD45.1^-$ $CD90.1^-$) recipients by i.p. injection. At the indicated time points, spleen, lymph nodes (inguinal, axillary, mesenterial, iliac), blood, and bone marrow were harvested and $CD45.1^+$ cells enriched by flow cytometric pre-enrichment ("speed enrichment") after red blood cell lysis. For speed enrichment a fluorescence trigger is set instead of a scatter trigger, cutting of particles negative for the enrichment marker. This trigger limits analysis complexity of the detected events to one parameter, thereby reducing consumption of electronic hardware resources and enabling dramatically increased sample flow rates in comparison to other flow cytometric approaches. Sorting time could thus be reduced up to 30-fold. After enrichment cells were stained and analyzed as described. Recruitment was calculated as:

$$Recruitment\ P14\ corrected\ \ [\%] = \left(1 - \frac{\frac{OT1}{P14} infected}{\frac{OT1}{P14} naive}\right) * 100$$

$$\text{or}\, Recruitment\ \ [\%] = \left(1 - \frac{OT1\ count\ infected}{OT1\ count\ naive}\right) * 100$$

Hemisplenectomy

Hemisplenectomy was performed as previously described [6]. Briefly, laparotomy was performed on anesthetized mice at day 8 p.i. with Lm-N4/T4 by a left subcostal incision of the skin and the peritoneum. The spleen was mobilized and approximately one-third of the spleen was ligated and removed. The wound on the remaining spleen was cauterized. Peritoneum and skin were closed by surgical stitches. The obtained spleen sample was placed in RPMI (10% FCS, 0.025% L-glutamine, 0.1% HEPES, 0.001% gentamycin, and 0.002% streptomycin) with Heparin to prevent coagulation until further processing.

Acknowledgments: This work was supported by the 'European Research Council starting grant' (949719 – SCIMAP) to V.R.B. and the Deutsche Forschungsgemeinschaft (DFG, German Research Foundation) – SFB 1054 (Projects B9 and B15, Project ID – 210592381) and GRK 2668 (Project B1 – Project ID: 435874434) to V.R.B. and D.H.B.
Open access funding enabled and organized by Projekt DEAL.

Conflict of interest: The authors declare no commercial or financial conflict of interest.

Author contributions: V.R.B., L.K. designed and supervised the study. V.R.B., L.K. and J.L. wrote the manuscript. J.L., A.M., I.A., M.B. and L.K. conducted experiments. D.H.B. contributed to the study design.

Ethics approval: All animal experiments were approved by the District Government of Upper Bavaria (Department 5-Environment, Health and Consumer Protection) and performed in accordance with national guidelines.

Data availability statement: The data that support the findings of this study are available from the corresponding author upon reasonable request.

Peer review: The peer review history for this article is available at https://publons.com/publon/10.1002/eji.202250009

References

1 **Nikolich-Žugich, J., Slifka, M. K. and Messaoudi, I.**, The many important facets of T-cell repertoire diversity. *Nat. Rev. Immunol.* 2004. **4**: 123–132.

2 **Huster, K. M., Busch, V., Schiemann, M., Linkemann, K., Kerksiek, K. M., Wagner, H. and Busch, D. H.**, Selective expression of IL-7 receptor on memory T cells identifies early CD40L-dependent generation of distinct CD8+ memory T cell subsets. *Proc. Natl. Acad. Sci.* 2004. **101**: 5610–5615.

3 **Joshi, N. S., Cui, W., Chandele, A., Lee, H. K., Urso, D. R., Hagman, J., Gapin, L. et al.**, Inflammation directs memory precursor and short-lived effector CD8+ T cell fates via the graded expression of T-bet transcription factor. *Immunity* 2007. **27**: 281–295.

4 **Kaech, S. M., Tan, J. T., Wherry, E. J., Konieczny, B. T., Surh, C. D. and Ahmed, R.**, Selective expression of the interleukin 7 receptor identifies

© 2022 The Authors. *European Journal of Immunology* published by Wiley-VCH GmbH

effector CD8 T cells that give rise to long-lived memory cells. *Nat. Immunol.* 2003. **4**: 1191–1198.

5 **Hikono, H., Kohlmeier, J. E., Takamura, S., Wittmer, S. T., Roberts, A. D. and Woodland, D. L.**, Activation phenotype, rather than central–or effector–memory phenotype, predicts the recall efficacy of memory CD8+ T cells. *J. Exp. Med.* 2007. **204**: 1625–1636.

6 **Grassmann, S., Mihatsch, L., Mir, J., Kazeroonian, A., Rahimi, R., Flommersfeld, S., Schober, K. et al.**, Early emergence of T central memory precursors programs clonal dominance during chronic viral infection. *Nat. Immunol.* 2020. **21**: 1563–1573.

7 **Johnnidis, J. B., Muroyama, Y., Ngiow, S. F., Chen, Z., Manne, S., Cai, Z., Song, S. et al.**, Inhibitory signaling sustains a distinct early memory CD8+ T cell precursor that is resistant to DNA damage. *Sci Immunol* 2021. **6**: eabe3702.

8 **Ferreira, D. P., Silva, J. G., Wyss, T., Marraco, S. A. F., Scarpellino, L., Charmoy, M., Maas, R. et al.**, Central memory CD8+ T cells derive from stem-like Tcf7hi effector cells in the absence of cytotoxic differentiation. *Immunity* 2020. **53**: 985–1000.e1011.

9 **Ozga, A. J., Moalli, F., Abe, J., Swoger, J., Sharpe, J., Zehn, D., Kreutzfeldt, M. et al.**, pMHC affinity controls duration of CD8+ T cell– DC interactions and imprints timing of effector differentiation versus expansion. *J. Exp. Med.* 2016. **213**: 2811–2829.

10 **Zehn, D., Lee, S. Y. and Bevan, M. J.**, Complete but curtailed T-cell response to very low-affinity antigen. *Nature* 2009. **458**: 211–214.

11 **Busch, D. H. and Pamer, E. G.**, T cell affinity maturation by selective expansion during infection. *J. Exp. Med.* 1999. **189**: 701–710.

12 **Day, E. K., Carmichael, A. J., Ten Berge, I. J., Waller, E. C., Sissons, J. P. and Wills, M. R.**, Rapid CD8+ T cell repertoire focusing and selection of high-affinity clones into memory following primary infection with a persistent human virus: human cytomegalovirus. *J. Immunol.* 2007. **179**: 3203–3213.

13 **Kim, C., Wilson, T., Fischer, K. F. and Williams, M. A.**, Sustained interactions between T cell receptors and antigens promote the differentiation of CD4+ memory T cells. *Immunity* 2013. **39**: 508–520.

14 **Savage, P. A., Boniface, J. J. and Davis, M. M.**, A kinetic basis for T cell receptor repertoire selection during an immune response. *Immunity* 1999. **10**: 485–492.

15 **Williams, M. A. and Bevan, M. J.**, Effector and memory CTL differentiation. *Annu. Rev. Immunol.* 2007. **25**: 171–192.

16 **van Heijst, J. W., Gerlach, C., Swart, E., Sie, D., Nunes-Alves, C., Kerkhoven, R. M., Arens, R. et al.**, Recruitment of antigen-specific CD8+ T cells in response to infection is markedly efficient. *Science* 2009. **325**: 1265–1269.

17 **ElTanbouly, M. A. and Noelle, R. J.**, Rethinking peripheral T cell tolerance: checkpoints across a T cell's journey. *Nat. Rev. Immunol.* 2021. **21**: 257–267.

18 **Kurts, C., Sutherland, R. M., Davey, G., Li, M., Lew, A. M., Blanas, E., Carbone, F. R. et al.**, CD8 T cell ignorance or tolerance to islet antigens depends on antigen dose. *Proc. Natl. Acad. Sci.* 1999. **96**: 12703–12707.

19 **Schietinger, A., Delrow, J. J., Basom, R. S., Blattman, J. N. and Greenberg, P. D.**, Rescued tolerant CD8 T cells are preprogrammed to reestablish the tolerant state. *Science* 2012. **335**: 723–727.

20 **Salaman, M. R. and Gould, K. G.**, Breakdown of T-cell ignorance: The tolerance failure responsible for mainstream autoimmune diseases? *J Transl Autoimmun* 2020. **3**: 100070.

21 **Theofilopoulos, A. N., Kono, D. H. and Baccala, R.**, The multiple pathways to autoimmunity. *Nat. Immunol.* 2017. **18**: 716–724.

22 **Hogquist, K. A., Jameson, S. C., Heath, W. R., Howard, J. L., Bevan, M. J. and Carbone, F. R.**, T cell receptor antagonist peptides induce positive selection. *Cell* 1994. **76**: 17–27.

23 **King, C. G., Koehli, S., Hausmann, B., Schmaler, M., Zehn, D. and Palmer, E.**, T cell affinity regulates asymmetric division, effector cell differentiation, and tissue pathology. *Immunity* 2012. **37**: 709–720.

24 **Knudson, K. M., Goplen, N. P., Cunningham, C. A., Daniels, M. A. and Teixeiro, E.**, Low-affinity T cells are programmed to maintain normal primary responses but are impaired in their recall to low-affinity ligands. *Cell Rep.* 2013. **4**: 554–565.

25 **Buchholz, V. R., Flossdorf, M., Hensel, I., Kretschmer, L., Weissbrich, B., Gräf, P., Verschoor, A. et al.**, Disparate individual fates compose robust CD8+ T cell immunity. *Science* 2013. **340**: 630–635.

26 **Gerlach, C., Rohr, J. C., Perié, L., van Rooij, N., Van Heijst, J. W., Velds, A., Urbanus, J. et al.**, Heterogeneous differentiation patterns of individual CD8+ T cells. *Science* 2013. **340**: 635–639.

27 **Pircher, H., Moskophidis, D., Rohrer, U., Bürki, K., Hengartner, H. and Zinkernagel, R. M.**, Viral escape by selection of cytotoxic T cell-resistant virus variants in vivo. *Nature* 1990. **346**: 629–633.

28 **Enouz, S., Carrié, L., Merkler, D., Bevan, M. J. and Zehn, D.**, Autoreactive T cells bypass negative selection and respond to self-antigen stimulation during infection. *J. Exp. Med.* 2012. **209**: 1769–1779.

29 **Grassmann, S., Pachmayr, L. O., Leube, J., Mihatsch, L., Andrae, I., Flommersfeld, S., Oduro, J. et al.**, Distinct surface expression of activating receptor Ly49H drives differential expansion of NK cell clones upon murine cytomegalovirus infection. *Immunity* 2019. **50**: 1391–1400.e1394.

30 **Grassmann, S., Sun, J. C. and Buchholz, V. R.**, *Retrogenic Color-Barcoding for Fate Mapping of Single Innate Lymphocytes Natural Killer (NK) Cells*. Springer 2022. 117–127.

31 **Williams, M. A., Ravkov, E. V. and Bevan, M. J.**, Rapid culling of the CD4+ T cell repertoire in the transition from effector to memory. *Immunity* 2008. **28**: 533–545.

32 **Richard, A. C., Lun, A. T., Lau, W. W., Göttgens, B., Marioni, J. C. and Griffiths, G. M.**, T cell cytolytic capacity is independent of initial stimulation strength. *Nat. Immunol.* 2018. **19**: 849–858.

33 **Daniels, M. A., Teixeiro, E., Gill, J., Hausmann, B., Roubaty, D., Holmberg, K., Werlen, G. et al.**, Thymic selection threshold defined by compartmentalization of Ras/MAPK signalling. *Nature* 2006. **444**: 724–729.

34 **Koehli, S., Naeher, D., Galati-Fournier, V., Zehn, D. and Palmer, E.**, Optimal T-cell receptor affinity for inducing autoimmunity. *Proc. Natl. Acad. Sci.* 2014. **111**: 17248–17253.

Full correspondence: Veit R. Buchholz and Lorenz Kretschmer
e-mail: veit.buchholz@tum.de; lorenz.kretschmer@tum.de

Received: 19/5/2022
Revised: 2/11/2022
Accepted: 29/11/2022
Accepted article online: 2/12/2022

© 2022 The Authors. *European Journal of Immunology* published by Wiley-VCH GmbH